Permanent Magnet Synchronous Motor (PMSM) for Aerospace Servomechanisms: Proposal of a Lumped Model for Prognostics

Permanent Magnet Synchronous Motor (PMSM) for Aerospace Servomechanisms: Proposal of a Lumped Model for Prognostics

Pier Carlo Berri, Matteo D.L. Dalla Vedova, Paolo Maggiore, Matteo Scanavino
Department of Mechanical and Aerospace Engineering
Politecnico di Torino
Torino, Italy
matteo.dallavedova@polito.it

***Abstract*—Prognostics and health management of electromechanical actuators (EMA) must rely on affordable and representative simulation models to be effective in predicting the evolution of failures, so to identify them before they occur through the assessment of monitored parameters, leading to on-spot maintenance operations. In the last years, electromechanical actuators (EMA) and the related modelling and monitoring issues are subject to a rising attention because of the design of next generation aircraft, based on the More Electric paradigm. In fact, especially in aeronautical fields (such as primary flight control systems), electromechanical actuators are progressively replacing traditional hydraulic and pneumatic systems because of their effectiveness and performances and, then, they are becoming safety-critical actuation devices: for prognostics and health management purposes of EMA, reliable and representative simulation models are needed in order to identify failures. In view of the above, this work proposes a multi-domain numerical simulation model of EMA, putting special attention on the fidelity of the numerical modelling of the inverter and of the related electromagnetic aspects; in particular, authors' research is focused on the modelling of the Permanent Magnet Synchronous Motor (PMSM), also known as Sinusoidal Brushless Motor. The choice of the multi-domain simulation is essential in order to enhance the behaviors of the said PMSM model and to overcome shortcomings related to the simplifying hypotheses that are typically considered in numerical models, which are commonly used also for prognostic analyses of electromechanical actuators.**

Keywords-PMSM, Electromechanical Actuator (EMA), Prognostics, PHM, Numerical Model

I. INTRODUCTION

In the last few years, the interest in brushless motors has increased because of their advantages compared with traditional brushed motors. The need of improvement in the design of electric motors was first reported during high altitude strategic bombing in World War II: in fact, at about 30000 ft, a rapid brush wear occurred [1-3]. Later on, during space exploration, the brush problem became crucial due to the outgassing phenomena. Brushless motors have been designed to overcome the brushed motor disadvantages: the electronic commutation, which is made possible by using electronic switches, replaces the mechanical commutation based on carbon made brushes. These latter need a periodic maintenance because of their wear; moreover, the mechanical commutation limits the maximum motor speed, since the brushes must be pushed against the collector ring by a spring. Brushless motors overcome these limitations and allow the motor operation even in the vacuum space, eliminating the production of sparks as well as allowing for higher motor speed range, faster motor dynamic response due to the motor weight reduction, better thermal performance and longer lifetime operation [1]. For aerospace applications, [2] presents preferred reliability practices for the selection criteria of the electric motor and remarks that brushless motors are the best all-around type of motors. Many different types of brushless motors have been developed: they are presented in [3]; this work will focus on the Permanent Magnet Synchronous Brushless Motors (PMSM) rather than Brushless DC Motors (BDCM). These motors have both a permanent magnet on the rotor and they require an alternating stator current to produce a constant motor torque. The back electromotive force and phase current waveforms are the main differences between the two machines: sinusoidal for PMSM and trapezoidal for BDCM; for this reason, the PMSM produces a smoother torque even near zero speed and is best suited for precise actuation systems. This study shows the preliminary results of our research activity focused on the numerical modelling of the PMSM for electromechanical aerospace actuation systems for future diagnostic and prognostic applications.

Then, progressive short-circuit and static eccentricity failure conditions are implemented in the proposed PMSM model. Furthermore, the developed model takes into account dry friction and it overcomes the typical limitations (e.g. simplifying assumptions such as the superposition of the effects) which are unable to assess nonlinear effects arising from failure conditions. This purpose is achieved by means of a multi-domain numerical method (e.g. Simulink Simscape and Sim Power System for the PWM controller and three phase circuit modelling) which allows the development of simulation algorithms properly sensitive to faults.

II. EM FLIGHT CONTROL ACTUATORS

Flight control systems allow controlling the aircraft dynamics: this is made possible by means of the proper actuation of the flight control surfaces.

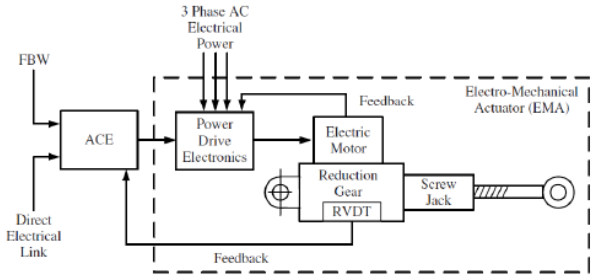

Fig. 1: Schematic of the considered EMA system

The aerodynamic forces, exerted on the flight control surfaces, will result in the aircraft rotation around one of the three body axes; in the last decades, flight control actuators were generally hydromechanical or electrohydraulic but, especially in recent years, the electromechanical systems are gradually asserting (e.g. UAVs, secondary or stand-by systems). Indeed, with respect to hydraulic systems, EMAs offer many advantages: overall weight is reduced, maintenance is simplified and hydraulic fluids, which are often contaminant, flammable or polluting, can be eliminated. For these reasons, as reported in [4], the use of actuation systems based on EMAs is quickly increasing in several fields of aerospace technology.

In Fig. 1, an electromechanical actuator scheme, for primary flight control, is presented. The EMA system is composed by:

- an actuator control electronics (ACE) that closes the feedback loop, by comparing the commanded position (FBW) with the actual one; it elaborates the corrective actions and generates the reference current (I_{ref});
- a Power Drive Electronics (PDE) that regulates the electrical power from the aircraft electrical system to the electric motor;
- an electric three-phase brushless motor;
- a gear reducer that decreases the motor angular speed and increases its mechanical torque;
- a system that converts rotary motion into linear motion: ball screws or roller screws are usually preferred over lead screws since they achieve a much higher mechanical efficiency;

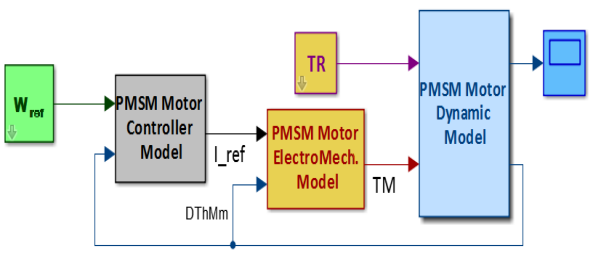

Fig. 2: Block diagram of the EMA numerical model

- a network of sensors that are used to close the feedback loops (current, motor speed and angular position) controlling the whole actuation system (reported in Fig.1 as RVDT).

III. Proposed PMSM Numerical Model

The authors' models, according to [5], implement the motor features only (rotor speed control loop and related reference current controller, pulse-width modulation (PWM) inverter, electromagnetic model of the stator circuit and related electromechanical model, internal sensors and considered faults).

The proposed model is shown in Fig. 2 and is composed by five subsystems:

- W_{ref}: input block that generates the reference motor speed;
- *PMSM Motor Controller Model*: it simulates the actuator control electronics closing the feedback loops and generating the reference current Iref;
- *PMSM Motor ElectroMech. Model*: it simulates the power drive electronics and the sinusoidal PMSM electromagnetic behaviour. Furthermore, it evaluates the mechanical torque developed by the electrical motor as a function of the voltages generated by the three-phase electrical regulator;
- *PMSM Motor Dynamic Model*: it simulates the motor mechanical behaviour by means of a nonlinear second order dynamical system;
- *TR*: input block that simulates the external load acting on the rotor shaft.

These numerical models also consider the electrical noise acting on the signal lines [4], the rotor bearings dry friction and the limit switches to constrain the maximum actuator travel [6].

A. Electromagnetic Model

The PMSM model is the development of the previous work carried out for the trapezoidal brushless motor BLDC [7]. A Circuital Model with Detailed Inverter (CMDI) has been implemented: the physical data used to implement these numerical algorithms and to run the corresponding simulations are referred to the TC 40 0.32 01 Tetra Compact sinusoidal brushless motor (as reported in Table 1).

TABLE I. Motor Data

Nominal voltage	48	[V]
Phase-phase resistance	1.10	[Ω]
Phase-phase inductance	0.72	[mH]
Torque constant	0.094	[Nm/A_{pp}]
Back-EMF constant	0.0544	[V_{pp}/A_{pp}]
Stall Torque	0.34	[Nm]
Rotor Inertia	0.047	[kg cm^2]

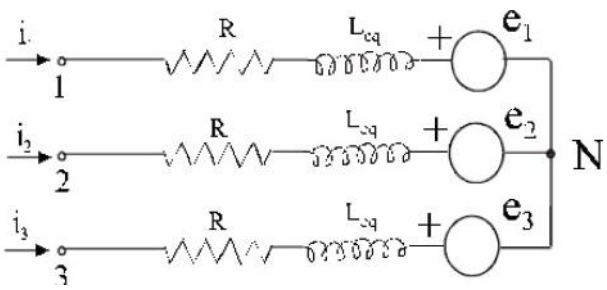

Fig. 3: Three-phase stator circuit

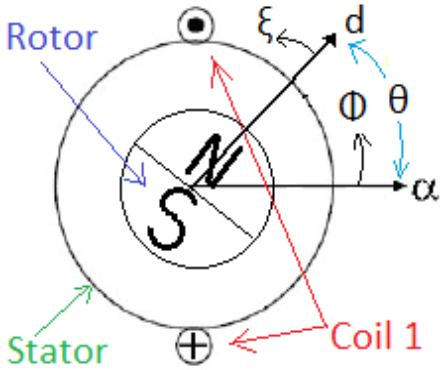

Fig. 4: Brushless Reference systems

Main PMSM The PMSM model is the development of the previous work carried out for the trapezoidal brushless motor BLDC [7]. A Circuital Model with Detailed Inverter (CMDI) has been implemented: the physical data used to implement these numerical algorithms and to run the corresponding simulations are referred to the TC 40 0.32 01 Tetra Compact sinusoidal brushless motor (as reported in Table 1).

The three-phase stator circuit is shown in Fig. 3. Each phase line is characterized by the same resistance R and the same inductance L_{eq}; moreover, the back electromotive forces e_1, e_2 and e_3 are introduced: they are related to the time derivative of the magnetic flux λ_m. The layout of the numerical model is similar to the BLDC model shown in [7] but, in this case, sinusoidal functions are used to describe the back electromotive forces and currents.

Three different reference systems are introduced to study the PMSM (as shown in Fig. 4):

- $\alpha - \beta$ *axes*: it is a stationary reference system where the α axis is fixed on the PMSM stator and it is defined by starting from the symmetrical axis of the phase 1. The β axis is perpendicular to α axis so that a right handed Cartesian system is obtained. The angle Φ is used as a polar coordinate to describe angles along the stator starting from the α axis;
- *d – q axes*: it is a rotating reference system with the rotor. The d axis points to the north pole line, while the q axis is perpendicular to the d axis. The angle ξ is a polar coordinate describing the angles along the rotor, starting from the d axis;
- *Three-phase reference system*: it is a stationary reference system where the axes (1, 2 and 3) fall into line with the three-phase windings of the motor: the axes are out of phase by 120° and the 1-axis corresponds to the α axis.

The relative angle between the stator and the rotor axes is θ. Applying Kirchhoff's law on each line it results that:

$$V_{1n} = Ri_1 + L_{eq}\,(di_1/dt) + e_1 \tag{1}$$

$$V_{2n} = Ri_2 + L_{eq}\,(di_2/dt) + e_2 \tag{2}$$

$$V_{3n} = Ri_3 + L_{eq}\,(di_3/dt) + e_3 \tag{3}$$

Moreover, for a balanced three-phase circuit:

$$i_1 + i_2 + i_3 = 0 \tag{4}$$

The motor torque is obtained from the power balance; it can be written as the superposition of the contribution of the three motor phases:

$$T_m = \sum_{j=1}^{3} i_j K_{ej} \tag{4}$$

which is equivalent, referred to $d - q$ axes, to [8]:

$$T_m = 3/2\ P\ \lambda_m\ i_q \tag{5}$$

where P and λ_m are the pole pair number and the magnetic flux respectively.

B. Clarke and Park Transformations

In order to obtain the three-phase reference currents from the reference i_q current, Park and Clarke transformations are employed (as described in [9]).

The transformation from a three-phase reference system into a two-phase system is commonly known as Clarke transformation:

$$\begin{bmatrix} i_\alpha \\ i_\beta \end{bmatrix} = [B] \begin{bmatrix} i_1 \\ i_2 \\ i_3 \end{bmatrix} \tag{6}$$

where [B] is the Clarke matrix:

$$[B] = \begin{bmatrix} 1 & -1/2 & -1/2 \\ 0 & \sqrt{3}/2 & -\sqrt{3}/2 \end{bmatrix} \tag{7}$$

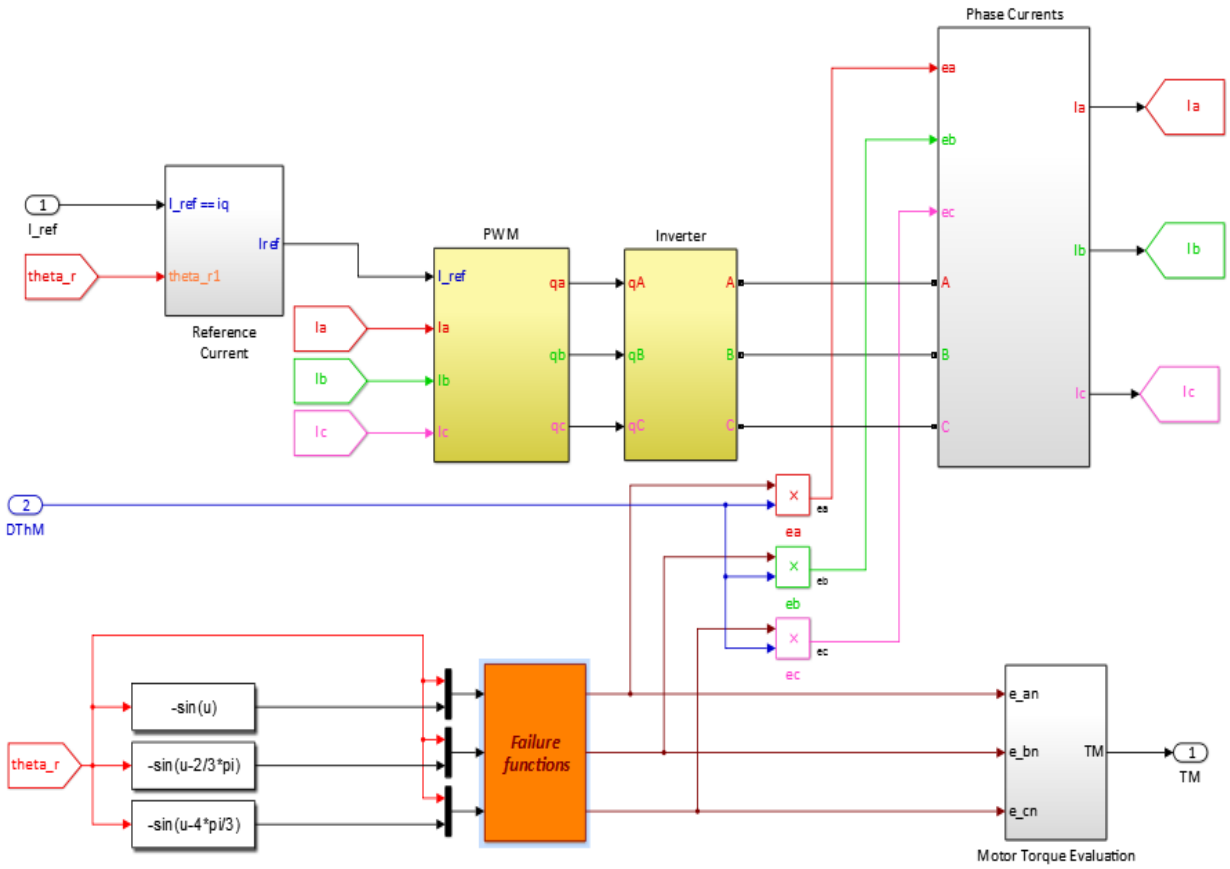

Fig. 5: PMSM Electromechanical Model subsystem

Park transformation allows converting α – β axes into *d* – *q* axes:

$$\begin{bmatrix} i_d \\ i_q \end{bmatrix} = [\mathrm{A}] \begin{bmatrix} i_\alpha \\ i_\beta \end{bmatrix} \tag{8}$$

where [A] is the Park matrix:

$$[\mathrm{A}] = \begin{bmatrix} \cos\theta & \sin\theta \\ -\sin\theta & \cos\theta \end{bmatrix} \tag{9}$$

The reference current (I_{ref}) is obtained from the PMSM Motor controller: a reference motor torque is turned into the reference current by using the motor torque constant k_t.

C. *PMSM Electromechanical Model*

The subsystem in Fig. 5 models a three-phase circuit: it receives, as input, the reference current Iref, the electrical angle and the rotor mechanical speed and position. The reference current subsystem (shown in Fig. 6) generates the reference sinusoidal currents for a three-phase circuit: the iq and id reference currents are set equal to the reference current Iref and zero respectively. The inverse Park and Clarke transformation matrices are implemented in order to obtain the corresponding three-phase reference currents.

The PWM, Inverter, Phase Currents and Motor Torque subsystems are the same as in [7], implemented in the Circuital Model with Detailed Inverter model. On the left bottom of Fig. 5 we can notice the normalized back electromotive forces, which are sinusoidal functions of the electric angle.

The back electromotive forces are obtained by multiplying the normalized BEMFs and the motor angular speed. The Failure Functions subsystem implements the short circuit and static eccentricity failure as shown in [10].

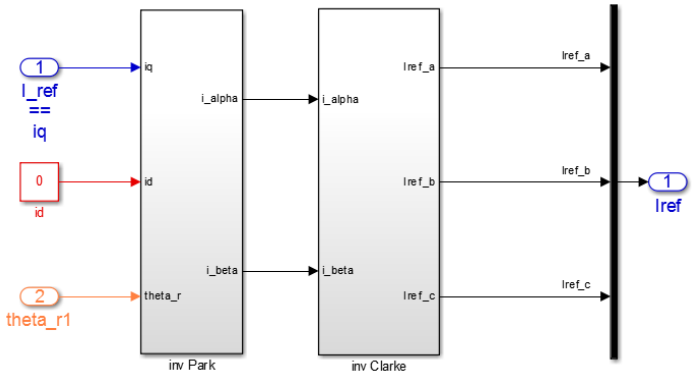

Fig. 6: Three-phase reference currents

D. *PMSM Speed Controller*

The motor control is achieved by means of a PID speed controller [11]: the input speed error is used to define the reference torque, which is turned into the reference current I_{ref}. The derivative term acts on the signal error, properly filtered, in order to ensure the stability of the entire system: a low-pass-filter is added to the derivative line for this purpose. The integral contribution is achieved with the anti-windup filter, which allows the desaturation of the integral term when the reference torque reaches the maximum value allowed. The three gains of the said PID PMSM speed controller are shown in Table 2.

TABLE II. MAIN PMSM DATA

Kp	0.025	[Nm/rad/s]
Ki	0.235	[Nm/rad]
Kd	10^{-6}	[Nm/rad/s^2]

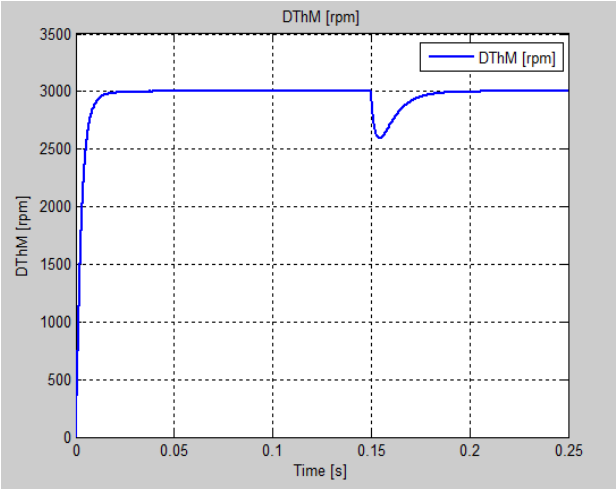

Fig. 7: PMSM motor speed time history

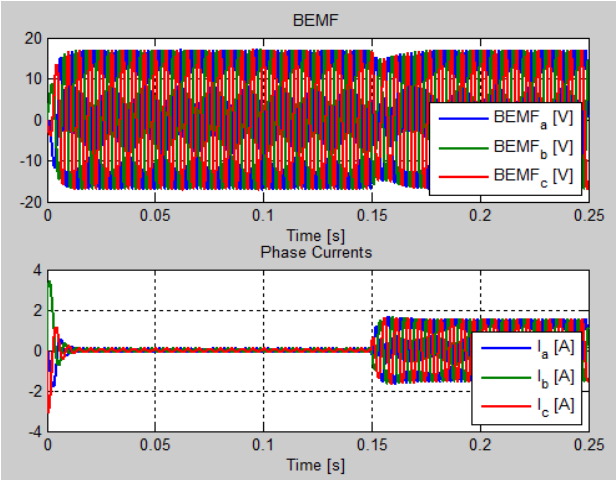

Fig. 8: BEMFs and phase currents

IV. RESULTS

In this section, in order to explain the performance of the proposed numerical model, the motor response to a reference speed is presented, in load conditions. The inverter over-modulation is shown at high reference motor speed.

A. *Nominal Conditions*

The reference speed is set equal to the nominal motor speed (3000 rpm). An external load (50% of the stall torque) is applied at time t = 0.15*s*.

Fig. 7 shows the motor speed time history, while in Fig. 8 the BEMFs and the actual three-phase currents are shown. It can be noticed that the phase currents increase when the external load is applied; at the same time, a reduction in the BEMFs is visible, due to the proportional relationship between the motor speed and BEMFs. In Fig. 9 the sinusoidal waveform of the actual three phase currents and the reference ones are shown. The motor torque time history is shown in Fig. 10.

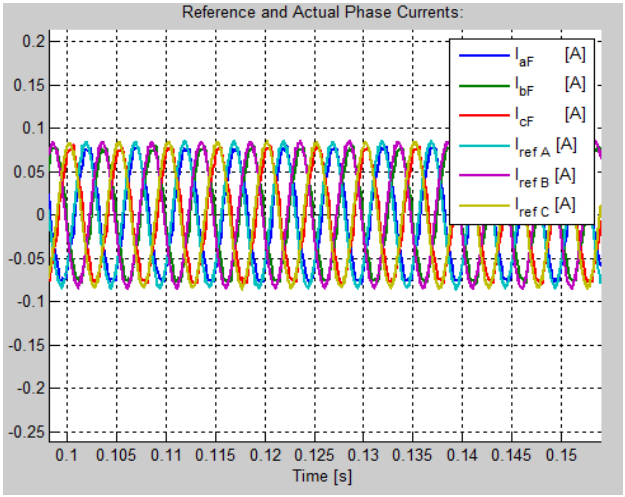

Fig. 9: PMSM reference and actual phase currents

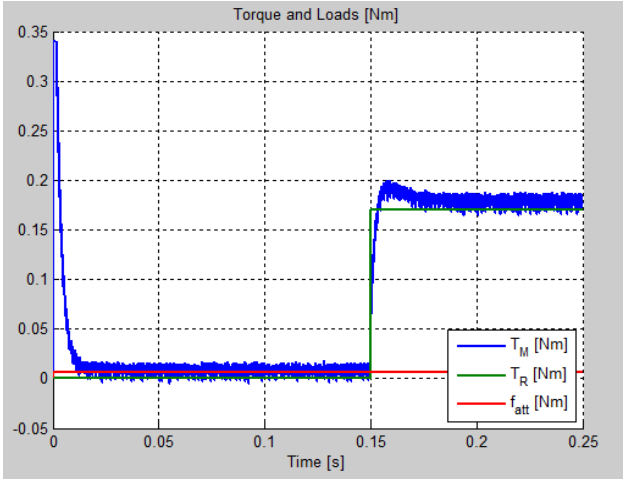

Fig. 10: PMSM motor torque TM, external load TR and friction torque f_{att} time history

B. *Inverter Over-Modulation Case*

Different reference motor speeds, ranging from the nominal speed to the maximum speed, have been considered (3000, 4500, 4800, 4900, 4950 and 5000 rpm). We have noticed the phase currents (Fig. 11) and voltages distortion when the reference speed reaches the maximum allowable value (5000 rpm), resulting in higher motor speed and torque fluctuations. The Fast Fourier Transform (FFT) of the actual A-three-phase current in Fig. 12 shows that, when the maximum speed is reached, the 5th and the 7th harmonics of the dominant frequency appear, as reported in [10] and shown in Fig. 13. At high speed the motor behaviour is out of the linear region: in fact, the peak phase voltage value (28.49 V) is greater than the expected value (24 V) from a 48 V inverter. To avoid this problem, the direct control of the motor in the $d - q$ axes should be useful.

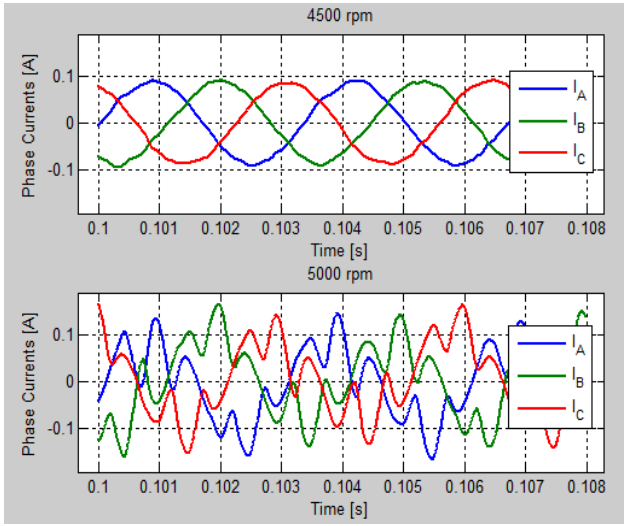

Fig. 11: Phase currents at 4500 and 5000 rpm

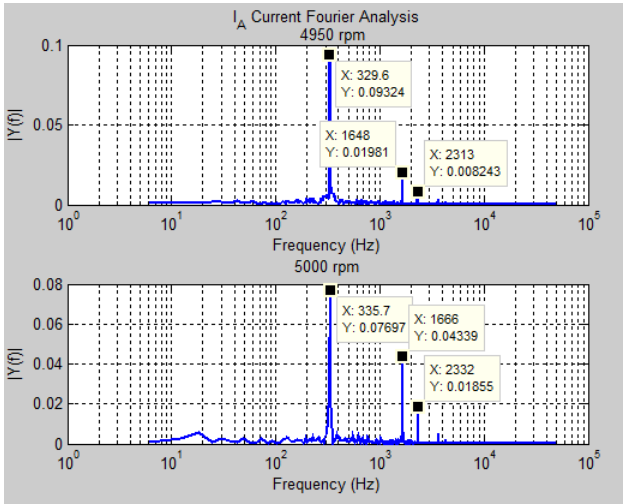

Fig. 12: FFT of A-phase current for 4950 and 5000 rpm

C. *Short Circuit and eccentricity faults*

The reference speed is set equal to the nominal motor speed (3000 rpm). An external load (50% of the stall torque) is applied at time t = 0.15s.

The use of this EMA model for prognostic analyses requires the ability to simulate a number of different fault modes. In this paragraph we focus on two electrical fault modes, namely partial phase short circuit [7] and static rotor eccentricity [4, 5].

The short circuit fault is implemented by modifying the values of resistance, inductance and back-EMF coefficient of one phase as a function of the fraction of non faulty windings of the corresponding phase N_1, N_2, N_3:

$$R_j = R\,N_j \tag{10}$$

$$L_j = L\,N_j^2 \tag{11}$$

$$K_{ej} = K_e\,N_j \tag{12}$$

for j = 1, 2, 3.

The static eccentricity fault is modelled as in [4], by modulating the back-EMF coefficients as a function of the local air gap width.

The upper part of Fig. 14 shows the id and iq currents: iq is directly proportional to the motor torque, while id should be equal to zero. A small positive value of the id is due to the hysteresis current control of the model, which will be replaced by a direct d – q control. In the lower part of Fig. 14 is shown the FFT of the reference phase current IA*. The failure is responsible for an asymmetrical behaviour of the motor and affects the appearance 3rd subharmonic of the dominant frequency of IA* under failure conditions.

The effect of an eccentricity fault condition (ζ = 0.4) is represented in Figure 15. This failure mode has an evident effect on the quadrature current i_q, where it triggers the appearance of the second subharmonic.

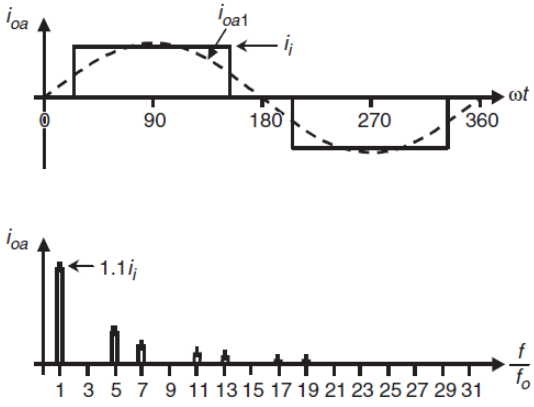

Fig. 13: Inverter over-modulation: AC output current time history (upper) and AC output current spectrum

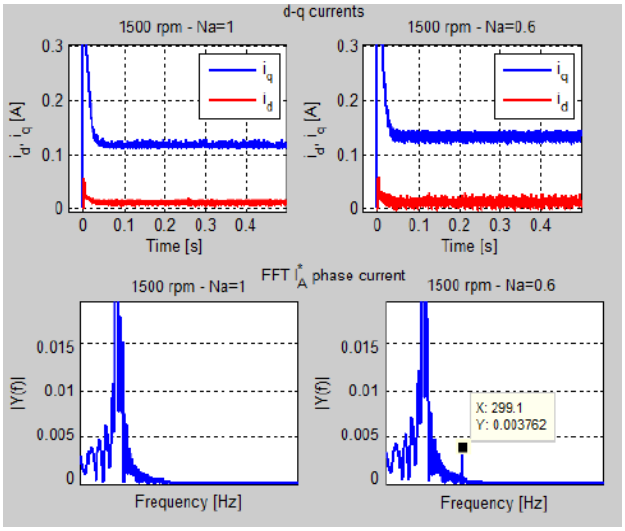

Fig. 14: Effect of partial short circuit of phase A (right) compared to nominal conditions (left)

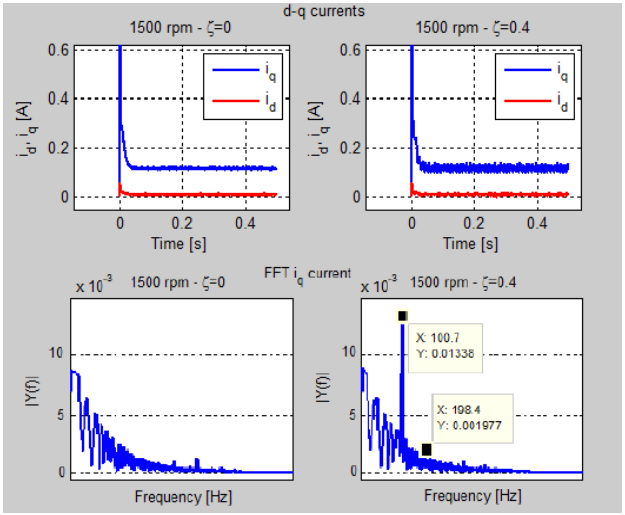

Fig. 15: Effect of eccentricity fault(right) compared to nominal conditions (left)

V. Conclusions

The numerical modelling of the electromechanical actuator using permanent magnet synchronous motor has been developed. The model was created in Matlab/Simulink environment. The Park and the Clarke transformations were introduced to describe the three-phase reference currents. The sinusoidal waveform of the normalized back electromotive force was introduced in order to describe the correct motor behavior and evaluate the total motor torque.

The PMSM motor control was developed imposing the reference quadrature current i_q and setting the direct current id equal to zero, as it normally does not contribute to the motor torque generation.

In order to improve the developed model, some suggestions are given:

- The Hysteresis Control will be replaced with the *d* – *q* axes direct control, in order to avoid the phase voltage and current distortions at high rotor speed.
- The failure conditions will be studied with greater detail. Demagnetization failure will be added in order to expand the considered failure modes.
- A simplified model of the actuator will be developed in order to monitor the motor actual behavior. This solution will be interesting for future diagnostic and prognostic applications.

Acknowledgment

The authors wish to thank professor Iustin Radu Bojoi for his support in the development of this work.

References

[1] Midwest Research Institute – NASA, Brushless DC Motors, January 1975.

[2] NASA Practice No. PD-ED-1229, Selection of electric motors for aerospace applications.

[3] P. Pillay, R. Krishnan, "Application Characteristics of Permanent Magnet Synchronous and Brushless dc Motors for Servo Drives", IEEE Transactions on industry applications, vol. 21, no. 5, September/October 1991.

[4] D. Belmonte, M. D. L. Dalla Vedova, P. Maggiore, "New prognostic method based on spectral analysis techniques dealing with motor static eccentricity for aerospace electro-mechanical actuators", WSEAS Transactions On Systems, vol. 14, 2015.

[5] "D. Belmonte, M.D.L. Dalla Vedova, P. Maggiore, Electromechanical servomechanisms affected by motor static eccentricity: Proposal of fault evaluation algorithm based on spectral analysis techniques", Safety and Reliability of Complex Engineered Systems (Proceedings of ESREL 2015), CRC Press, September 2015, pp. 2365-2372.

[6] L. Borello, M. D. L. Dalla Vedova, G. Jacazio, M. Sorli, "A Prognostic Model for Electro-hydraulic Servovalves", Annual Conference of the Prognostics and Health Management Society, San Diego, CA, USA, 2009.

[7] L. Pace, M. D. L. Dalla Vedova, P. Maggiore, S. Facciotto, "Numerical methods for the electromagnetic modelling of actuators for primary and secondary flight controls", Computational Science and Systems Engineering, vol. 58, pp. 126-133, 2016.

[8] P. Moreton, Industrial Brushless Servomotors, Newnes, January 2000.

[9] S. Chattopadhyay, M. Mitra, S.Sengupta, Electric Power Quality, Springer, Chapter 12.

[10] M. D. L. Dalla Vedova, P. Maggiore, L. Pace, A. Desando, "Evaluation of the correlation coefficient as a prognostic indicator for electromechanical servomechanism failures", International Journal of Prognostics and Health Management, vol. 6, no. 1, 2015.

[11] M. H. Rashid, Power electronics handbook, 3rd ed., Butterworth-Heinemann, 2011.